AAV-mediated gene therapy in Dystrophin-Dp71 deficient mouse leads to blood-retinal barrier restoration and oedema reabsorption

Ophélie Vacca, Hugo Charles-Messance, Brahim El Mathari, Abdoulaye Sene, Peggy Barbe, Stéphane Fouquet, Jorge Aragón, Marie Darche, Audrey Giocanti-Aurégan, Michel Paques, et al.

AAV-mediated gene therapy in Dystrophin-Dp71 deficient mouse leads to blood-retinal barrier restoration and oedema reabsorption

Ophélie Vacca[1,2,*], Hugo Charles-Messance[1], Brahim El Mathari[1], Abdoulaye Sene[3], Peggy Barbe[1], Stéphane Fouquet[1], Jorge Aragon[1,4], Marie Darche[1], Audrey Giocanti-Aurégan[1,5], Michel Paques[1,6], José-Alain Sahel[1,6], Ramin Tadayoni[1,7], Cecilia Montañez[4], Deniz Dalkara[1] and Alvaro Rendon[1]

[1]Sorbonne Universités, UPMC Univ Paris 06, INSERM, CNRS, Institut de la Vision, 17 rue Moreau, 75012 Paris, France; [2]Neuroscience Paris-Saclay Institute (NeuroPSI) - CNRS UMR 9197 - Université Paris-Sud, Cognition & Behavior, rue Claude Bernard, 91405 Orsay cedex, France; [3]Department of Ophthalmology, Therapeutic, 1635 Washington Ave, Saint Louis, MO, USA 63103; [4]Department of Genetics & Molecular Biology, CINVESTAV: Research Centre for Advanced Studies, IPN, Av. Instituto Politécnico Nacional 2508, C.P. 07360 México, Mexico; [5]Ophthalmology Department, Avicenne Hospital, 125 Rue De Stalingrad, Bobigny, France; [6]CHNO des Quinze-Vingts, DHU Sight Restore, INSERM-DHOS CIC, 28 rue de Charenton, 75012 Paris, France; [7]Ophthalmology Dept, Hôpital Lariboisière, AP-HP, Univ Paris Diderot, France.

*To whom correspondence should be addressed at: Email: ophelie.vacca@gmail.com

Key Words

Gene therapy; AAV; Müller glial cell; Dystrophin Dp71; Blood-retinal barrier

Abstract

Dystrophin-Dp71 being a key membrane cytoskeletal protein, expressed mainly in Müller cells that provide a mechanical link at the Müller cell membrane by direct binding to actin and a transmembrane protein complex. Its absence has been related to blood-retinal barrier (BRB) permeability through delocalization and down-regulation of the AQP4 and Kir4.1 channels (1). We have previously shown that the adeno-associated virus (AAV) variant, ShH10, transduces Müller cells in the Dp71-null mouse retina efficiently and specifically (2,3). Here, we use ShH10 to restore Dp71 expression in Müller cells of Dp71 deficient mouse to study molecular and

functional effects of this restoration in an adult mouse displaying retinal permeability. We show that strong and specific expression of exogenous Dp71 in Müller cells leads to correct localization of Dp71 protein restoring all protein interactions in order to re-establish a proper functional BRB and retina homeostasis thus preventing retina from oedema. This study is the basis for the development of new therapeutic strategies in dealing with diseases with BRB breakdown and macular oedema such as diabetic retinopathy (DR).

Introduction

Dp71 belongs to the dystrophin superfamily, and is a short product of the DMD gene, located on the X chromosome, involved in Duchenne muscular dystrophy (DMD) (4). Dp71—a membrane-bound cytoskeletal protein (5)—plays an important role in glial and vascular functions in the retina. It forms, with other proteins called dystrophin associated proteins (DAPs), a dystrophin glycoprotein complex (DGC) establishing a molecular link between the cytoskeleton and the surrounding extracellular matrix. It contributes to anchor ion/water channels and receptors in specific membrane fractions. DAPs include dystroglycan, syntrophin, dystrobrevin, and sarcoglycan. These are found in association either with Dp71 or utrophin—dystrophin autosomal homolog—(6) and play both structural and intracellular signal transduction roles. Dp71, absent from skeletal muscle, is predominant in the central nervous system (CNS). In the retina, all products of the DMD gene are expressed through the activation of internal promoters for each dystrophin. Dp71 is mainly localized in Müller cells and more specifically in their inner endfeet, around retinal vessels, closely related to the blood retinal barrier (BRB) (6,7).

Tight junctions located between endothelial cells of retinal blood vessels, pericytes and Müller glial cell endfeet, form the BRB. Indeed, Müller cells participate in the maintenance and functioning of the BRB (8–10). Previous work on mice had shown that the deletion of Dp71 causes a BRB breakdown suggesting a crucial role of Dp71 in BRB integrity (1). Indeed, genetic inactivation of Dp71 (11) alters b-dystoglycan, potassium and water channels' (Kir4.1 and AQP4) distribution along Müller glial cells that results in a disregulation of water transport through Müller cells (1). Thus, Dp71 associated with b-dystoglycan is required for proper clustering and precise membrane localization of Kir4.1 and AQP4 channels (12,13). From now

on, we will call Dp71, b-dystoglycan, Kir4.1 and AQP4 of Müller glial cell endfeet, the Dp71-dependent protein complex.

Vascular leakage and impaired fluid absorption from the retinal tissue across the glio-vascular interface are major pathogenic events of BRB breakdown (14). Both pathological mechanisms are stimulated by the absence of Dp71. Nevertheless, the Dp71-null retina is not naturally oedematous since we did not measure any increase in the retinal thickness of this mouse model (2). In the clinic, BRB breakdown of retinal detachment is a major cause of vision loss. Moreover, BRB breakdown in macular oedema is an important complication occurring in uveitis, diabetic retinopathy (DR), and macular telangiectasia (MacTel2) (15). The BRB breakdown is a symptom, which is the core of many important eye pathologies. In previous studies, we have shown in both retinal detachment (1) and Irvine Gass syndrome mouse model that BRB breakdown leads to Dp71 down-regulation (L.Siqueiros Marquez and A.Giocanti-Aurégan, manuscript in preparation). Thus, the absence of Dp71 causes BRB breakdown and conversely BRB breakdown induces Dp71 down-regulation making of Dp71-null mouse, a good animal model to study BRB permeability and of the Dp71 protein, an ideal therapeutic target to elaborate novel treatments for ocular diseases related to BRB breakdown (patent No 08 305381.9, 2008; patent No EP09305608.3, 2010).

In this study, we developed a gene transfer to restore Dp71 expression in the Dp71 deficient mouse and thereby increasing retinal vascular permeability. To this aim, we used adeno-associated virus (AAV) to deliver Dp71 transgene to the major cell type involved in BRB maintenance: Müller glial cells. AAV has become the most promising ocular gene delivery vehicle over the past 15 years. Its low immunogenicity, ability to infect the majority of retinal cells, and long-term transgene expression make the virus a safe and very efficient gene delivery vector. We recently tested an AAV capsid variant, ShH10 that efficiently and specifically transduces Müller glial cells from the vitreous of the Dp71-null mouse (2,16). Here, we employed this variant to restore Dp71 in Müller glial cells of Dp71 deficient mice. This virus was intraviteally injected to 8-weeks-old Dp71- null mice. GFP fluorescence was observed by fundus images and retinal thickness was measured by optical coherence tomography (SD-OCT).

We found that Dp71 expression leads to proper localization of this protein in Müller glial cell endfeet and consecutively leads to the up-regulation of several genes coding for transmembrane and ECM proteins related to Dp71. Furthermore, proteins of the Dp71-

dependent complex re-localized to their proper compartments after treatment. Importantly, restoration of Dp71 leads to the total reabsorption of oedema caused by an intravitreal saline injection of Dp71-null mice as well as restoration of normal BRB permeability. Our data strongly suggest that Dp71 restoration is able to alleviate all symptoms related to the absence of the Dp71 protein despite the fact that intervention was made after development. These finding open promising avenues in the development of gene based therapies in diseases with permeable BRB where Dp71 is down-regulated.

Results

ShH10 delivers Dp71 to Müller glial cells

To restore Dp71 expression, we cloned the complete murine Dp71 sequence from exon 63 to exon 79 (GenBank: JN900253.1) without splicing and GFP under the control of a ubiquitous CBA promoter. To obtain a bicistronic expression of both genes, we inserted the viral 2A peptide between coding sequences, on GFP C-terminal and Dp71 N-terminal (17). Thus, we produced an AAV with ShH10 capsid and GFP-2A-Dp71 transgene (referred to: ShH10-GFP-2A-Dp71), since ShH10 targets specifically and efficiently Müller glial cells in Dp71-null mice (2,13).

One microliter stock containing 1.8 1010 particles of ShH10-GFP-2A-Dp71 was injected intravitreally to 8-weeks-old Dp71-null mice. Control eyes received vehicle (PBS) or ShH10-GFP injection. Fundus imaging showed GFP expression across transduced retinas (Fig. 1A–D). We obtained a similar transduction pattern and the same GFP intensity using ShH10-GFP-2ADp71 or ShH10-GFP (Fig. 1E and F). Both viruses had the same intense transduction pattern only targeting Müller glial cells (Fig. 1E and F).

Quantitative RT-PCR and protein analysis of Dp71-treated eyes

Two months after ShH10-GFP-2A-Dp71 injection, RNA and protein were extracted from treated retinas by Trizol method. In parallel, we performed qRT-PCR and Western Blot analysis to evaluate expression levels of Dp71-dependent complex, utrophin (dystrophin homolog, present in Müller glial cell endfeet) and other ECM genes coding for proteins located in Müller glial cell endfeet binding Dp71-dependent protein complex (Tables 1 and 2).

We observed that Dp71 mRNA and protein were significantly over-expressed in the Dp71-null retinas in respect to wild-type Dp71 levels (Figs 2, 3A and C). Thus, ShH10-GFP-2A-Dp71 restores Dp71 expression in Müller glial cells.

It is known that Dp71 is associated with b-dystroglycan, AQP4 and Kir4.1 clustering in Müller glial cell endfeet. This Dp71-dependent protein complex is linked to the inner limiting membrane by the interaction of laminin and agrin with a-dystroglycan (13,18). Therefore, we analysed the expression levels of all these mRNA, and we found that AQP4, Kir4.1, laminin and agrin mRNA in ShH10-GFP-2A-Dp71-treated retinas were significantly higher compared to both wild-type and Dp71-null retinas (Fig. 2). At the protein level, we observed that b-dystroglycan was also over-expressed in ShH10-GFP-2A-Dp71-treated retinas (Fig. 3B and D). Full-length utrophin messenger, dystrophin autosomal homolog expressed in Müller cell endfeet, was slightly up-regulated. These results suggested that Dp71 overexpression induced the stimulation of a Dp71-dependent transcriptome (Fig. 2).

It is known that Müller glial cells become activated in response to retinal damage or cellular defects. This activation is characterized by the induction of glial fibrillary acidic protein (GFAP). To verify if AAV injection or Dp71 over-expression induce Müller cell gliosis, we quantified GFAP mRNA levels. We found that the amount of GFAP messenger did not increase in treated retinas versus controls (Fig. 2).

Relocalization of Dp71-dependent protein complex

In wild-type Müller glial cells, we have already established that Kir4.1, AQP4 and b-dystroglycan co-clustered in the endfeet of these cells. In the absence of Dp71, these three proteins are distributed along Müller glial cells (13). Here, we investigated the localization of these proteins after Dp71 restoration. We isolated Müller glial cells and immunostained with the following antibodies: anti-glutamine synthetase or anti-GFAP to identify Müller glial cells, H4 (pan-specific antibody) to localize exogenous Dp71, anti-b-dystroglycan, anti-AQP4 and anti-Kir4.1. We observed that the restoration of Dp71 rescued the localization at the Müller glial cell endfeet of Dp71, b-dystroglycan, AQP4 and Kir4.1 (Fig. 4A). We also performed retinal cryosections of Dp71- null-treated mice and we confirmed the relocalization of Dp71, b-dystroglycan, AQP4 and Kir4.1 at the Müller glial cell endfeet and around vessels (19) (Fig. 4B and Supplementary Material, Fig. S2). Thus, Dp71 expression through ShH10 allowed relocalization of the Dp71-dependent protein complex at the inner limiting membrane and at

the glio-vascular interface forming the BRB of Dp71-null mouse retina, which was the first step prior to rescue Müller glial cell functions. Moreover, we remarked a morphological difference between Dp71-null and Dp71-restored MGC endfeet. Whereas Dp71-null MGC endfeet looked looser and spread-out, Dp71-restored MGC endfeet looked compact and clustered. Therefore, MGC endfeet seemed to recover their wild-type morphology (Fig. 4A) (13).

Reabsorption of induced Oedema in Dp71-null mouse retinas

Although, in a previous work, we have shown that intact retinal layers were thinner in the Dp71-null mice compared to wildtype retinas (2). Here, we observed that two months after an intravitreal injection of PBS, the retinas of Dp71-null mice presented a significant thickness increase in the whole retina with respect to the wild-type mice (Fig. 5B). The thickness was increased in the inner retina (Fig. 5C) whereas the ONL and photoreceptor segments were unchanged (Supplementary Material, Fig. S1). These results suggested that Dp71-null mouse is more sensitive to retinal oedema than wild-type mouse and that oedema cannot be reabsorbed due to deficient Müller glial cell function. However, upon restoration of Dp71 through ShH10- GFP-2A-Dp71 treatment, Dp71-null retinas did not show oedema in response to PBS injection (Fig. 5B and C). This absence of thickness variation in ShH10-GFP-2A-Dp71-treated retinas after PBS injection suggests that Dp71 expression helps the oedema reabsorption by restoring the role of Müller glial cells in retinal homeostasis (Fig. 5B and C).

Restoration of blood-retinal barrier permeability

We have demonstrated in previous studies that the absence of Dp71 in Müller glial cells is accompanied by an increased permeability of the blood-retinal barrier (BRB) (1) and that the VEGF (Vascular Endothelial Growth Factor), a vascular permeability factor is also increased (20). We assessed retinal vascular permeability, in wild-type and vehicle-injected Dp71-null mice in comparison to Dp71-null mice treated with ShH10-GFP-2ADp71. Vascular permeability was evaluated using the Evans blue-dye technique (21). We showed that restoration of Dp71 by viral-mediated expression can rescue normal vascular permeability (Fig. 6 left). We also quantified VEGF-A mRNA expression, and we showed that Dp71 restoration leads to VEGF-A mRNA restoration to the wild-type expression level (Fig. 6 right). This observation is in agreement with the postulated direct correlation existing between Dp71 in Müller glial cells

and BRB permeability (1). Thus, we can say that Dp71 plays a pivotal role in retinal homeostasis and in BRB permeability.

Discussion

AAV-mediated Dp71 expression (ShH10-GFP-2A-Dp71) in Müller glial cells shows that it is possible to restore Dp71 expression and thereby, relocate Dp71-dependent protein complex. This in turn leads to normal retinal homeostasis, restoring BRB permeability and reabsorbing retinal oedema.

ShH10-GFP-2A-Dp71 leads to Dp71 expression in Müller glial cells deficient in Dp71. The expression level was 7-fold higher compared to wild-type Dp71 level. A similar result was obtained for Dp71-dependent genes or proteins as a/b-dystroglycan, AQP4, Kir4.1, laminins, agrin and utrophin (Figs 2 and 3). These high levels did not seem to cause any adverse effects.

In the present study, we have restored cDNA of the unspliced Dp71, called the Dp71d (22,23), thus eliminating any transcriptional regulation and therefore the expression of other Dp71 isoforms (24–29). However, Dp71 undergoes several alternative-splicing events. Restoration of others isoforms could allow the regulation of the Dp71-dependent complex expression. Therefore, it would be very interesting to study the functional effects of the restoration of each Dp71 isoform in the Dp71-null retina. We have demonstrated for the first time that Dp71 restoration in MGC re-establishes a normal BRB permeability proving that MGC recovered their ability to regulate the vascular permeability (Fig. 6) (8,9). This is most likely a result of the relocalization of potassium and water channels (Kir4.1 and AQP4) and of the consequent restoration of the water transport regulation through MGC.

We have shown that Dp71-null retina is more sensitive to needle injury than wild-type retina since a single saline intravitreous injection induce an increase of the inner retina thickness that persists at least two months after the injection (Fig. 5). The retinal thickness increase might be due to the deregulation of water transport associated with the K+ current in the Dp71-null MGC. The deregulation of water transport that results in the swelling of MGC when exposed to an osmotic stress (1) could lead in Dp71-null mice to retinal oedema. It is very difficult to develop macular oedema animal models because most experimental animals do not possess macula. Dp71-null retina does not naturally present retinal oedema (2)

whereas after a single intravitreal injection of saline solution, Dp71-null mice could be used as macular oedema animal model.

In addition, we have found that Dp71 restoration leads to the relocalization of Dp71, b-dystroglycan and potassium/water channels (Kir4.1/AQP4) in MGC endfeet at the inner limiting membrane (Fig. 4). The relocalization of this macromolecular complex could allow fluid reabsorption by the MGC, hence the decrease in the thickness of the retina corresponding to a reuptake of retinal oedema (Fig. 5). Moreover, we have previously shown that Dp71 by linking Kir4.1, and AQP4 allows the aggregation of these channels in “lipid raft” membrane domains (13). The aggregation in membrane microdomains of Kir4.1 and AQP4 channels in MGC is crucial for the functional coupling of these channels since these channels co-locate and support K+ and water transport in glial cells (30–34).

Based on the present data, we propose the following model for Dp71 restoration in Dp71-null mice. First, the ShH10-GFP-2A-Dp71 intravitreal injection induces Dp71 restoration in Müller glial cells. Second, Dp71 restoration allows Dp71-dependent protein complex up-regulation and relocalization in Müller glial cell endfeet at the ILM and around vessels. Finally, recovering a functional Dp71-dependent protein complex in Müller glial cell endfeet leads to BRB reinstatement and retinal oedema reabsorption. Knowing that Dp71 is downregulated in pathologies showing BRB breakdown, we highlighted that the successful Dp71 restoration is an important step forwards the development of new treatments for retinal diseases with symptoms of BRB breakdown and macular oedema such as DR.

Materials and Methods

Animals

The Dp71-null mice (11) was a kind gift from Pr David Yaffe and were produced by replacing, via homologous recombination, most of the first and unique exon of Dp71 and of a small part of Dp71 first intron with a sequence encoding a b-gal-neomycin-resistance chimeric protein (b-geo). In this mouse line, Dp71 expression is abolished without interfering with the expression of other products of the DMD gene. C57BL/6J mouse strain (JANVIER, France) was used as controls for this study. All animals used in this study were cared for and handled according to the ARVO Statement for the Use of Animals in Ophthalmic and Vision Research.

Generation and purification of AAV vectors

Recombinant AAVs were produced by the plasmid cotransfection method (35), and the resulting lysates were purified via iodixanol gradient ultracentrifugation as previously described (36). Briefly 40% iodixanol fraction was concentrated and buffer exchanged using Amicon Ultra-15 Centrifugal Filter Units. Vector stocks were then tittered for DNase-resistant vector genomes by real time PCR relative to a standard (37). Each vector contained a self-complimentary genome encoding the viral 2A peptide for bicistronic expression (17) of GFP and Dp71 under the control of a ubiquitous CBA promoter. The GFP-2ADp71 cDNA was synthesized by GENEWIZ, Inc. (USA) and cloned into an AAV plasmid (pTR-SB-smCBA) containing inverted terminal repeat (ITR) regions for the packaging of the interest sequence into ShH10 capsid. The vector was further modified with a single Y445F tyrosine to phenylalanine mutation for enhanced intracellular and nuclear trafficking (38), which was introduced into the ShH10 capsid plasmid using a site directed mutagenesis kit (QuikChange Lightning, Agilent Technologies).

Injections

Before vector administration, mice were anesthetized with ketamine (50 mg/kg) xylazine (10 mg/kg Rompum). Pupils were dilated by the ocular instillation of neosynephrine 5% Faure (Europhta) and mydriaticum 0,5% (Théa) eye drops. An ultrafine 30-gauge disposable needle was passed through the sclera, at the equator and next to the limbus, into the vitreous cavity. Injection of 1 ml stock containing 1.8 x 1010 particles of AAV was made with direct observation of the needle in the center of the vitreous cavity. Left eyes were injected and right eyes served as control.

Fundus photography

Fundus examinations were performed at one or two months after the intravitreal injection of ShH10 coding GFP or GFP-2ADp71 under the ubiquitous CAG promoter. Fundus photographs were obtained with a Micron III fundus camera. Mouse pupils were dilated by the application of neosynephrine (5%) and mydriaticum (0,5%) eye drops prior to imaging.

Optical Coherence Tomography

OCT was performed using an SD-OCT system (Bioptigen Inc., Durham, NC) (39). Hydration with normal saline was used to preserve corneal clarity. Volume analysis centered on the optic nerve head was performed, using 100 horizontal, raster, and consecutive B-scan lines, each one composed of 1200 A-scans. The volume size was 1.4 0.1 mm either side of the optic nerve. A custom software was used to generate the en face fundus image using reflectance information obtained from the OCT sections (volume intensity projection), so that the point-to-point correlation between OCT and fundus position was possible and accurate.

Müller glial cell isolation

The retinas were isolated and incubated in papain (Papain from Carica papaya, 10108014001, Roche) for 30 min at 37 C, followed by a washing step with saline (PBS) and a 10 min fixation step with 4% paraformaldehyde (PFA). After this step, the tissue pieces were shortly incubated in PBS supplemented with DNase I (160 U/ml; Invitrogen) and triturated by a pipette to obtain a suspension of isolated cells. The cells were stored at 4 C in serum-free minimum essential medium (Sigma) until use within three hours after isolation.

Immunostaining of isolated cells

Suspension of freshly dissociated Müller cells was distributed on glass slides and air-dried. Adherent cells are rehydrated with PBS, briefly fixed with 2% PFA, and permeabilized with PBS/0.1% Triton for 5 minutes. After 1 hour of saturation in PBS/0.1% Tween 20/3% normal growth factor (NGS)/1% bovine serum albumin (BSA), cells were incubated with primary antibody (Table 1) overnight at 4 C. After several washes with PBS/0.1% Triton, secondary antibodies (Interchim, France) coupled to Alexa were used diluted 1:500 in PBS for 1 h at room temperature. Glass slides were mounted with Fluorsave reagent (Calbiochem). Confocal microscopy was performed on an Olympus FV1000 laser-scanning confocal microscope. Images were acquired sequentially, line-by-line, in order to reduce excitation and emission crosstalk, step size was defined according to the Nyquist-Shannon sampling theorem. Exposure settings that minimized oversaturated pixels in the final images were used. Twelve bit Images were then processed with FIJI; Z-sections were projected on a single plane using maximum intensity under Z-project function and finally converted to 8- bit RGB color mode.

Table 1. Primary antibodies used for immunostaining and Western Blot

Protein	Species	References	Immunostaining	Western Blot	Source
Glutamin Synthetase	mouse	MAB302	1:2000	-	Millipore
GFAP	rabbit	Z0334	1:1000	-	Dako
Dystrophins (H4)	rabbit	-	1:1000	1:5000	Homemade by D.Mornet
Dystrophins	mouse	DYS2-CE	1:20	1:10	Novocastra
AQP4	rabbit	AQP-004	1:500	1:100	Alomone
Kir4.1	rabbit	APC-035	1:200	1:500	Alomone
β-dystroglycan	mouse	B-DG-CE	1:200	1:100	Novocastra
Utrophin (K7)	rabbit	-	-	1:500	Homemade by D.Mornet
Utrophin (DRP2)	mouse	DRP2CE	-	1:10	Novocastra
GFP	chicken	ab13970	1:500	-	Abcam
β-Actin	mouse	A2228	-	1:7500	Sigma

Western Blot analysis

Western blot analysis was performed as previously described (40). In brief, retinal protein extracts were resolved using NuPAGE Tris–Acetate 3–8% gradient gels (Invitrogen, France) and electrotransferred to polyvinylidene difluoride (PVDF) membranes according to the manufacturer's instructions. PVDF membranes were blocked in PBS containing 5% dry milk (BIORAD, Herts, UK) for 1 h at room temperature then incubated overnight at 4 C with the primary antibody in the same blocking buffer. Blots were then washed and incubated with the secondary antibody conjugated to horseradish peroxidase (Jackson Immunoresearch laboratories). Chemiluminescence was performed using ECL plus Western blotting detection system (GE Healthcare, Germany) and documented on film (GE Healthcare, Germany).

Quantitative RT-PCR analysis

Total RNA from retina was extracted using Trizol reagent (Invitrogen, France) according to the manufacturer's instructions. Reverse transcription was performed on 1 µg total RNA using SuperScript III and random hexamers (Invitrogen, France). PCR amplifications of cDNA were

performed using Master plus SYBR Green I (Roche Diagnostics, Germany) on a LightCycler instrument (Roche Products, Basel, Switzerland). PCR primers were designed using Primer3 software (41) (Table 2). For relative comparison, the Ct values of real-time PCR results were analysed using the ΔCt method according to the manufacturer's instructions. The amount of cDNA was normalized to the standard internal control obtained using primers for b-Actin.

Table 2. Primer sequences for quantitative RT-PCR

Name	Sense	Antisense
Dp71	ATGAGGGAACACCTCAAAGGCCACG	TCTGGAGCCTTCTGAGCTTC
Dystroglycan	CTTGAGGCGTCCATGCACT	GGCAATTAAATCCGTTGGAATGC
AQP4	CTTTCTGGAAGGCAGTCTCAG	CCACACCGAGCAAAACAAAGAT
Laminin alpha 1	CAGCGCCAATGCTACCTGT	GGATTCGTACTGTTACCGTCACA
Laminin gamma 3	CGGAGCCCTGCATCACAAA	AGCAAGGTCGTCCTCAAAGC
Kir4.1	CCGCGATTTATCAGAGC	AGATCCTTGAGGTAGAGGAA
Utrophin/exon1	GGATCTGGGAAAGCCTTTGGA	TCGTTCTGCCCATCATCAGG
GFAP	CCACCAAACTGGCTGATGTCTAC	TTCTCTCCAAATCCACACGAGC
Agrin	CACCGGGGACACTAGAATCTT	GAGCTACCATAGCAGGGCA
β-Actin	GCTCTTTTCCAGCCTTCCTT	CTTCTGCATCCTGTCAGCAA

Quantification of blood-retinal barrier permeability

Vascular permeability was quantified by measuring albumin leakage from blood vessels into the retina using the Evans blue method (21). Briefly, mice were anesthetized and Evans blue (45 mg/kg; Sigma-Aldrich, Germany) was injected through the penile vein (3). Blood samples were taken 3 h after injection of the dye and mice were perfused for 2 min via the left ventricle with a citrate buffer (0.05 M, pH 3.5) pre-warmed to 37°C. After perfusion, both eyes were enucleated and carefully dissected. Retinas were dried in a Speed-Vac for 5 h, weighed and the Evans blue dye was extracted by incubating the retina with 100 µl of formamide for 18 h at 70°C. Retinal supernatant was filtrated with Nanosep 30k omega tubes (VWR) at 14 000 g during 2 h at 4°C. Blood samples were centrifugated at 18 000 g during 15 min. Both supernatants were used to measure absorbance. A background-subtracted absorbance was determined by measuring each sample at both 620 nm (absorbance maximum for Evans blue) and 740 nm (absorbance minimum) (TECAN infinite M1000). Evans

blue concentration in the plasma and the retina was calculated from a standard curve of Evans blue in formamide. Blood-retinal barrier (BRB) permeability was expressed in microliter of Evans blue per gram of dry retina per hour (µl Evans blue x g dry retina-1 x h-1).

Data analysis

Results are expressed as mean 6 Standard Error of the Mean (SEM). Confocal stacks of 50 images were taken with the same settings. These images were Z projected and the fluorescence area was quantified with Fiji (Fiji Is Just ImageJ) software. Fluorescence data were then analysed using Mann Whitney U test with Prism 5 (GraphPad Software, San Diego, CA). P values < 0.05 accepted as statistically significant.

Acknowledgements

We acknowledge Mélissa Desrosiers for skillful technical assistance with AAV preparations.

Conflict of Interest statement. Conflict of Interest statement. AFM, CONACyT, ECOS Nord, Labex, AVOPH, ANR DysTher are public or non-commercial organizations. Allergan has offered an unrestricted grant to the laboratory used for this study. Authors also disclose the following Conflict of Interests with Commercial Entities: Ramin Tadayoni is a board member of and consultant for Alcon, Switzerland; Novartis, Switzerland; Allergan, USA; Bausch and Lomb, USA; Alimera, USA; Bayer, Germany; FCIZeiss, France; Thrombogenics, Belgium; Roche, Switzerland; Genentech, USA; Zeiss, Germany. He has received lecture fees from Alcon, USA; Bausch and Lomb, USA; Novartis, Switzerland; Allergan, USA; Bayer, Germany; Alimera, USA, Zeiss, Germany, and meeting expenses from Novartis, Switzerland; Alcon, Switzerland; Allergan, USA; Bausch and Lomb, USA; Bayer, Germany; Alimera, USA. Audrey Giocanti-Auregan is consultant for Allergan, USA; Bayer, Germany, and Novartis, Switzerland. She has received lecture fees from Novartis, Switzerland; Allergan, USA; Bayer, Germany, and meeting expenses from Novartis, Switzerland; Alcon, Switzerland; Allergan, USA; Bayer, Germany, and Alimera, USA.

Funding

This work was supported by (i) the Association Française contre les Myopathies (AFM) for a research project grant number 14853 to A.R. and (ii) a PhD grant number 14768 to O.V., (iii) Allergan INC., (iv) the Institut National de la Santé et de la Recherche Médicale (INSERM), (v) the French State program “Investissements d’Avenir” managed by the Agence Nationale de la Recherche [LIFESENSES: ANR-10-LABX-65], and (vi) EcosNord program number M11S02.

References

1. Sene, A., Tadayoni, R., Pannicke, T., Wurm, A., El Mathari, B., Benard, R., Roux, M.J., Yaffe, D., Mornet, D., Reichenbach, A. et al. (2009) Functional implication of Dp71 in osmoregulation and vascular permeability of the retina. PLoS One, 4, e7329.

2. Vacca, O., Darche, M., Schaffer, D.V., Flannery, J.G., Sahel, J.A., Rendon, A. and Dalkara, D. (2014) AAV-mediated gene delivery in Dp71-null mouse model with compromised barriers. GLIA, 62, 468–476.

3. Vacca, O., El Mathari, B., Darche, M., Sahel, J.A., Rendon, A. and Dalkara, D. (2015) Using adeno-associated virus as a tool to study retinal barriers in disease. J. Vis. Exp., 98, doi: 10.3791/52451

4. Bar, S., Barnea, E., Levy, Z., Neuman, S., Yaffe, D. and Nudel, U. (1990) A novel product of the Duchenne muscular dystrophy gene which greatly differs from the known isoforms in its structure and tissue distribution. Biochem. J., 272, 557–560.

5. Rapaport, D., Greenberg, D.S., Tal, M., Yaffe, D. and Nudel, U. (1993) Dp71, the nonmuscle product of the Duchenne muscular dystrophy gene is associated with the cell membrane. FEBS Lett., 328, 197–202.

6. Claudepierre, T., Mornet, D., Pannicke, T., Forster, V., Dalloz, C., Bolanos, F., Sahel, J., Reichenbach, A. and Rendon, A. (2000) Expression of Dp71 in Muller glial cells: a comparison with utrophin- and dystrophin-associated proteins. Invest. Ophthalmol. Vis. Sci., 41, 294–304.

7. Howard, P.L., Dally, G.Y., Wong, M.H., Ho, A., Weleber, R.G., Pillers, D.A. and Ray, P.N. (1998) Localization of dystrophin isoform Dp71 to the inner limiting membrane of the retina suggests a unique functional contribution of Dp71 in the retina. Hum. Mol. Genet., 7, 1385–1391.

8. Tout, S., Chan-Ling, T., Hollander, H. and Stone, J. (1993) The role of Muller cells in the formation of the blood-retinal barrier. Neuroscience, 55, 291–301.

9. Distler, C. and Dreher, Z. (1996) Glia cells of the monkey retina–II. Muller cells. Vision Res., 36, 2381–2394.

10. Tretiach, M., Madigan, M.C., Wen, L. and Gillies, M.C. (2005) Effect of Muller cell co-culture on in vitro permeability of bovine retinal vascular endothelium in normoxic and hypoxic conditions. Neurosci. Lett., 378, 160–165.

11. Sarig, R., Mezger-Lallemand, V., Gitelman, I., Davis, C., Fuchs, O., Yaffe, D. and Nudel, U. (1999) Targeted inactivation of Dp71, the major non-muscle product of the DMD gene: differential activity of the Dp71 promoter during development. Hum. Mol. Genet., 8, 1–10.

12. Connors, N.C. and Kofuji, P. (2002) Dystrophin Dp71 is critical for the clustered localization of potassium channels in retinal glial cells. J. Neurosci., 22, 4321–4327.

13. Fort, P.E., Sene, A., Pannicke, T., Roux, M.J., Forster, V., Mornet, D., Nudel, U., Yaffe, D., Reichenbach, A., Sahel, J.A. et al. (2008) Kir4.1 and AQP4 associate with Dp71- and utrophin-DAPs complexes in specific and defined microdomains of Muller retinal glial cell membrane. GLIA, 56, 597–610.

14. Cunha-Vaz, J.G. and Travassos, A. (1984) Breakdown of the blood-retinal barriers and cystoid macular edema. Surv. Ophthalmol., (Suppl. 28), 485–492.

15. Charbel Issa, P., Gillies, M.C., Chew, E.Y., Bird, A.C., Heeren, T.F., Peto, T., Holz, F.G. and Scholl, H.P. (2013) Macular telangiectasia type 2. Prog. Retin. Eye Res, 34, 49–77.

16. Klimczak, R.R., Koerber, J.T., Dalkara, D., Flannery, J.G. and Schaffer, D.V. (2009) A novel adeno-associated viral variant for efficient and selective intravitreal transduction of rat Muller cells. PLoS One, 4, e7467.

17. Trichas, G., Begbie, J. and Srinivas, S. (2008) Use of the viral 2A peptide for bicistronic expression in transgenic mice. BMC Biol., 6, 40.

18. Noel, G., Belda, M., Guadagno, E., Micoud, J., Klocker, N. and Moukhles, H. (2005) Dystroglycan and Kir4.1 coclustering in retinal Muller glia is regulated by laminin-1 and requires the PDZ-ligand domain of Kir4.1. J. Neurochem., 94, 691–702

19. Dalloz, C., Sarig, R., Fort, P., Yaffe, D., Bordais, A., Pannicke, T., Grosche, J., Mornet, D., Reichenbach, A., Sahel, J. et al. (2003) Targeted inactivation of dystrophin gene product Dp71: phenotypic impact in mouse retina. Hum. Mol. Genet., 12, 1543–1554.

20. El Mathari, B., Sene, A., Charles-Messance, H., Vacca, O., Guillonneau, X., Grepin, C., Sennlaub, F., Sahel, J.A., Rendon, A. and Tadayoni, R. (2015) Dystrophin Dp71 gene deletion induces retinal vascular inflammation and capillary degeneration. Hum. Mol. Genet., 24, 3939–3947.

21. Xu, Q., Qaum, T. and Adamis, A.P. (2001) Sensitive bloodretinal barrier breakdown quantitation using Evans blue. Invest. Ophthalmol. Vis. Sci., 42, 789–794.

22. Austin, R.C., Howard, P.L., D'Souza, V.N., Klamut, H.J. and Ray, P.N. (1995) Cloning and characterization of alternatively spliced isoforms of Dp71. Hum. Mol. Genet., 4, 1475–1483.

23. Aleman, V., Osorio, B., Chavez, O., Rendon, A., Mornet, D. and Martinez, D. (2001) Subcellular localization of Dp71 dystrophin isoforms in cultured hippocampal neurons and forebrain astrocytes. Histochem. Cell Biol., 115, 243–254.

24. Gorecki, D.C., Monaco, A.P., Derry, J.M., Walker, A.P., Barnard, E.A. and Barnard, P.J. (1992) Expression of four alternative dystrophin transcripts in brain regions regulated by different promoters. Hum. Mol. Genet., 1, 505–510

25. Lederfein, D., Levy, Z., Augier, N., Mornet, D., Morris, G., Fuchs, O., Yaffe, D. and Nudel, U. (1992) A 71-kilodalton protein is a major product of the Duchenne muscular dystrophy gene in brain and other nonmuscle tissues. Proc. Natl. Acad. Sci. U S A., 89, 5346–5350.

26. Austin, R.C., Fox, J.E., Werstuck, G.H., Stafford, A.R., Bulman, D.E., Dally, G.Y., Ackerley, C.A., Weitz, J.I. and Ray, P.N. (2002) Identification of Dp71 isoforms in the platelet membrane cytoskeleton. Potential role in thrombin-mediated platelet adhesion. J Biol. Chem., 277, 47106–47113.

27. Ceccarini, M., Rizzo, G., Rosa, G., Chelucci, C., Macioce, P. and Petrucci, T.C. (1997) A splice variant of Dp71 lacking the syntrophin binding site is expressed in early stages of human neural development. Brain Res. Dev. Brain Res., 103, 77–82.

28. Saint Martin, A., Aragon, J., Depardon-Benitez, F., SanchezTrujillo, A., Mendoza-Hernandez, G., Ceja, V. and Montanez, C. (2012) Identification of Dp71e, a new dystrophin with a novel carboxy-terminal end. FEBS J., 279, 66–77.

29. Tozawa, T., Itoh, K., Yaoi, T., Tando, S., Umekage, M., Dai, H., Hosoi, H. and Fushiki, S. (2012) The shortest isoform of dystrophin (Dp40) interacts with a group of presynaptic proteins to form a presumptive novel complex in the mouse brain. Mol. Neurobiol., 45, 287–297.

30. Higashi, K., Fujita, A., Inanobe, A., Tanemoto, M., Doi, K., Kubo, T. and Kurachi, Y. (2001) An inwardly rectifying K(þ) channel, Kir4.1, expressed in astrocytes surrounds synapses and blood vessels in brain. Am. J. Physiol. Cell Physiol., 281, C922–C931.

31. Kofuji, P., Ceelen, P., Zahs, K.R., Surbeck, L.W., Lester, H.A. and Newman, E.A. (2000) Genetic inactivation of an inwardly rectifying potassium channel (Kir4.1 subunit) in mice: phenotypic impact in retina. J. Neurosci., 20, 5733–5740.

32. Nagelhus, E.A., Horio, Y., Inanobe, A., Fujita, A., Haug, F.M., Nielsen, S., Kurachi, Y. and Ottersen, O.P. (1999) Immunogold evidence suggests that coupling of Kþ siphoning and water transport in rat retinal Muller cells is mediated by a coenrichment of Kir4.1 and AQP4 in specific membrane domains. GLIA, 26, 47–54.

33. Nielsen, O.B. and Clausen, T. (1997) Regulation of Na(þ)-Kþ pump activity in contracting rat muscle. J. Physiol., 503, 571–581.

34. Takumi, T., Ishii, T., Horio, Y., Morishige, K., Takahashi, N., Yamada, M., Yamashita, T., Kiyama, H., Sohmiya, K., Nakanishi, S. et al. (1995) A novel ATP-dependent inward rectifier potassium channel expressed predominantly in glial cells. J. Biol. Chem., 270, 16339–16346.

35. Grieger, J.C., Choi, V.W. and Samulski, R.J. (2006) Production and characterization of adeno-associated viral vectors. Nat. Protoc., 1, 1412–1428.

36. Choi, V.W., Asokan, A., Haberman, R.A. and Samulski, R.J. (2007) Production of recombinant adeno-associated viral vectors for in vitro and in vivo use. Curr. Protoc. Hum. Genet., Chapter 16:Unit 16.25. doi: 10.1002/ 0471142727.mb1625s78

37. Aurnhammer, C., Haase, M., Muether, N., Hausl, M., Rauschhuber, C., Huber, I., Nitschko, H., Busch, U., Sing, A., Ehrhardt, A. et al. (2012) Universal real-time PCR for the detection and quantification of

adeno-associated virus serotype 2-derived inverted terminal repeat sequences. Hum. Gene Ther. Methods, 23, 18–28.

38. Petrs-Silva, H., Dinculescu, A., Li, Q., Min, S.H., Chiodo, V., Pang, J.J., Zhong, L., Zolotukhin, S., Srivastava, A., Lewin, A.S. et al. (2009) High-efficiency transduction of the mouse retina by tyrosine-mutant AAV serotype vectors. Mol. Ther., 17, 463–471.

39. Berger, A., Cavallero, S., Dominguez, E., Barbe, P., Simonutti, M., Sahel, J.A., Sennlaub, F., Raoul, W., Paques, M. and Bemelmans, A.P. (2014) Spectral-domain optical coherence tomography of the rodent eye: highlighting layers of the outer retina using signal averaging and comparison with histology. PLoS One, 9, e96494.

40. Bordais, A., Bolanos-Jimenez, F., Fort, P., Varela, C., Sahel, J.A., Picaud, S. and Rendon, A. (2005) Molecular cloning and protein expression of Duchenne muscular dystrophy gene products in porcine retina. Neuromuscul. Disord., 15, 476–487.

41. Rozen, S. and Skaletsky, H. (2000) Primer3 on the WWW for general users and for biologist programmers. Methods Mol. Biol., 132, 365–386.

Figures

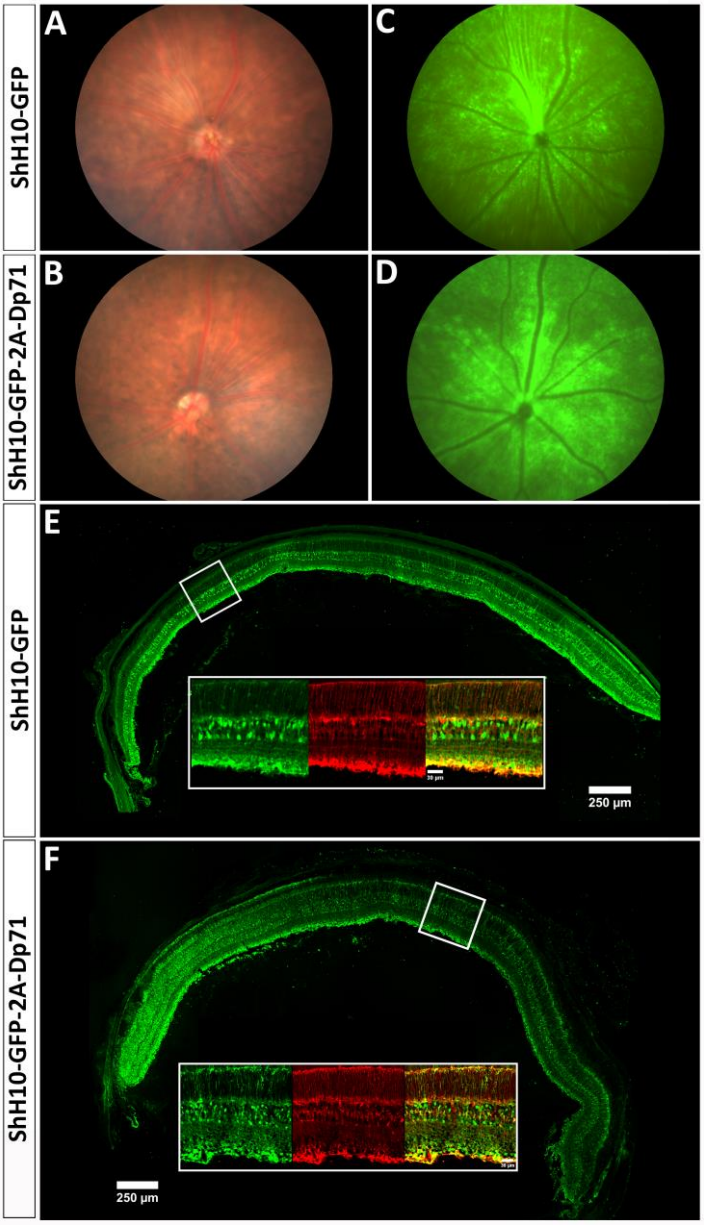

Figure 1. Retinal integrity and transduction efficiency. Fundus images of the Dp71-null retina 2 months after intravitreal injection of ShH10-GFP (A, C) or ShH10-GFP-2A-Dp71 (B, D) showed that both AAVs strongly transduced the whole retina (C, D). Confocal imaging (E, F) of an entire cryoslice (scale bar = 250 mm) showing the GFP expression (green) with both ShH10-GFP (E) and ShH10- GFP-2A-Dp71 (F) vectors and immunostaining of close-up images (white rectangle) with glutamine synthetase (red) to visualize the colocalization meaning that transduced cells are Müller cells with both vectors (scale bar = 30 mm).

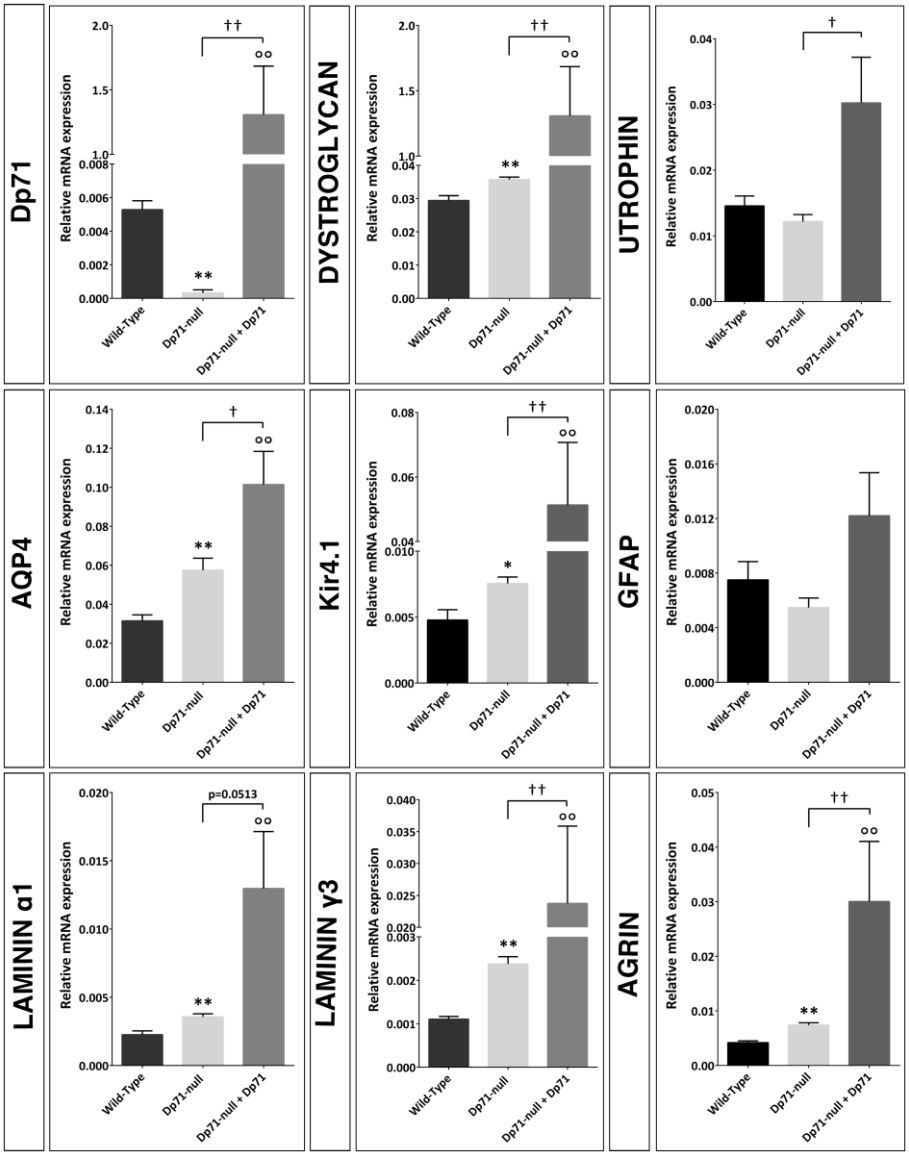

Figure 2. Dp71 mRNA over-expression leads to over-expression of mRNAs associated with Dp71. Quantitative RT-PCR showed an over-expression of Dp71, dystroglycans, AQP4, Kir4.1, agrin and laminins mRNAs in the treated Dp71-null mouse in comparison with the wild-type. Quantitative RT-PCR showed that the utrophin mRNA is slightly up-regulated while GFAP didn't show any variation. Bars represent means ± SEM for triplicate data points; n = 7. *P < 0.05, **P < 0.01 significant differences versus wild-type; P < 0.01 significant differences versus wild-type; † P < 0.05, ††P < 0.01 significant differences versus Dp71-null (Mann-Whitney test).

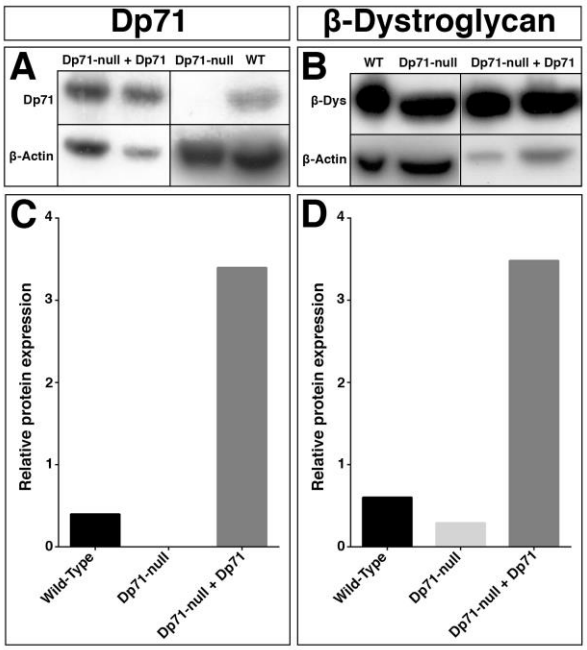

Figure 3. Dp71 and b-dystroglycan over-expression two months after intravitreal injection of ShH10-GFP-Dp71 in the Dp71-null mouse retina. Western blot and subsequent band density semi-quantification relative to b-actin of Dp71 (A, C) using H4 antibody and of b-dystroglycan (B, D).

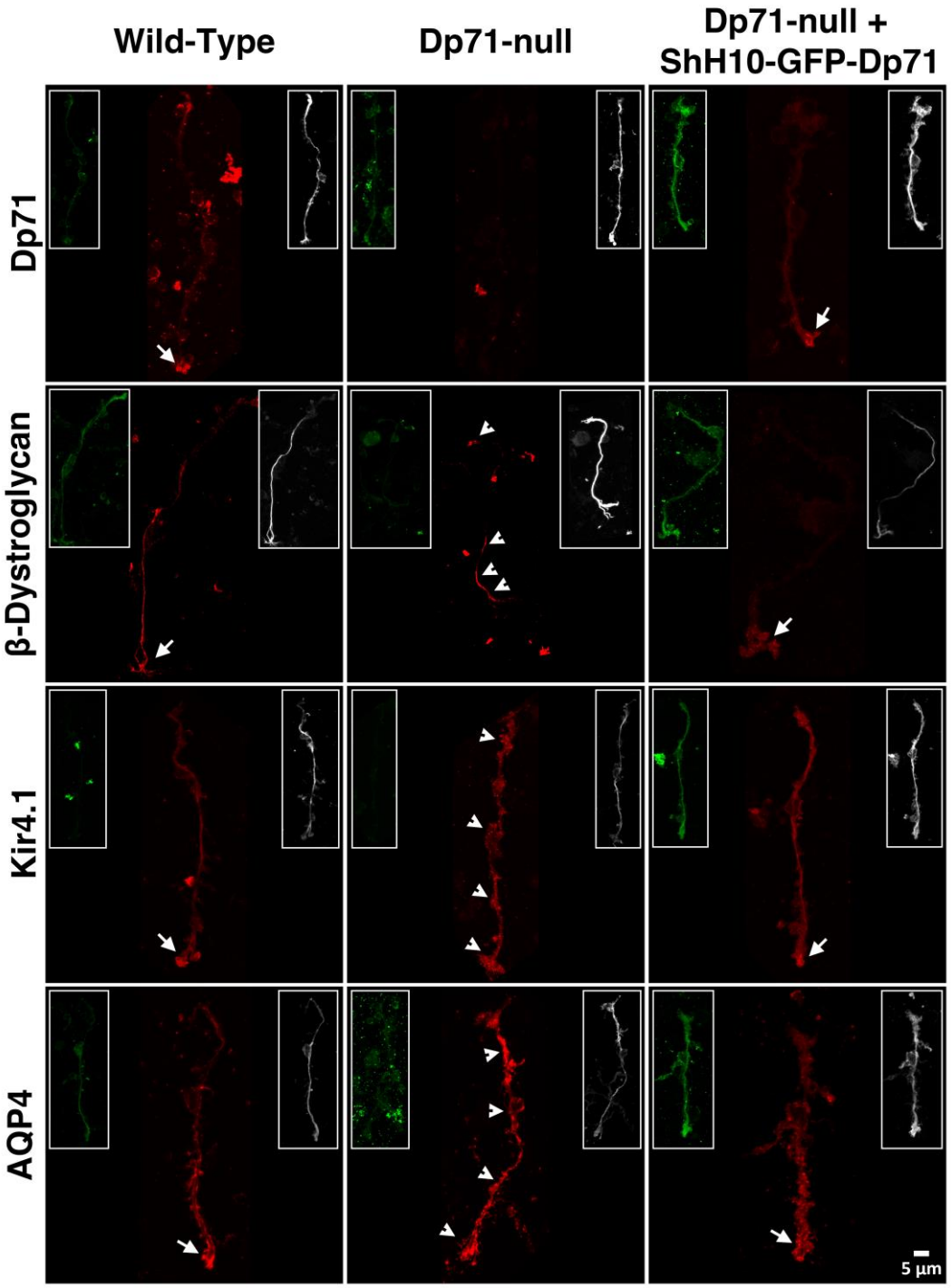
Wild-Type
Dp71-null
Dp71-null +
ShH10-GFP-Dp71
Dp71
β-Dystroglycan
Kir4.1
AQP4
5 µm

Fig.4A

Fig.4B 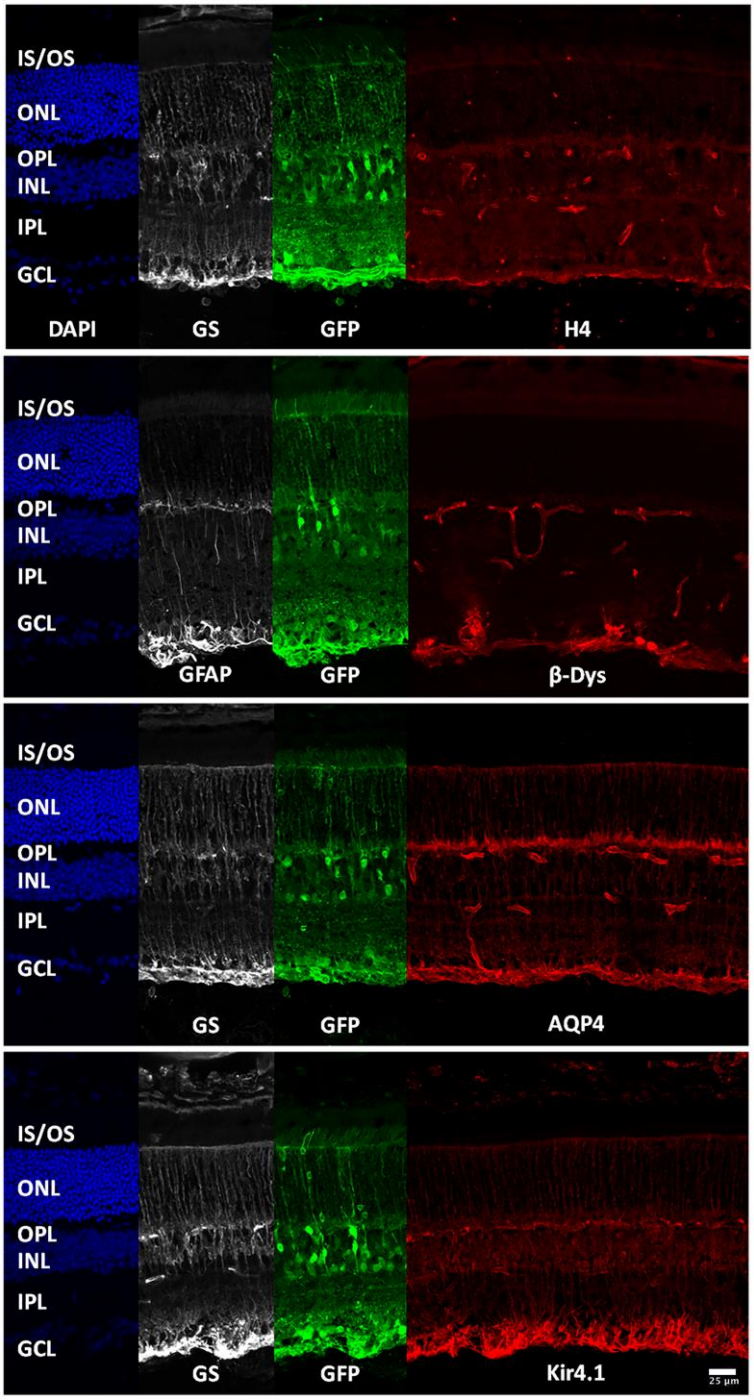

Figure 4. A. Relocalization of Dp71 and Dp71 related proteins in the Müller glial cells. Isolated Müller glial cells stained with GS antibody (grey), expressing GFP (green) and stained with H4 (red) showing Dp71 expression mainly located in the Müller glial cell endfeet (white arrows). Same observations were made for b-dystroglycan, potassium channel Kir4.1 and for water channel AQP4 (n = 4) (scale bar = 5 mm). B. Retinal cryosections of Dp71-null mice retinas after Dp71 restoration. Sections were labelled with DAPI (blue), glutamine synthetase (grey) or

GFAP (grey) to visualize Müller cells, GFP (green) to identify transduced cells, H4 to localize Dp71, b-dystroglycan, AQP4 and Kir4.1 (red) (scale bar = 25 mm).

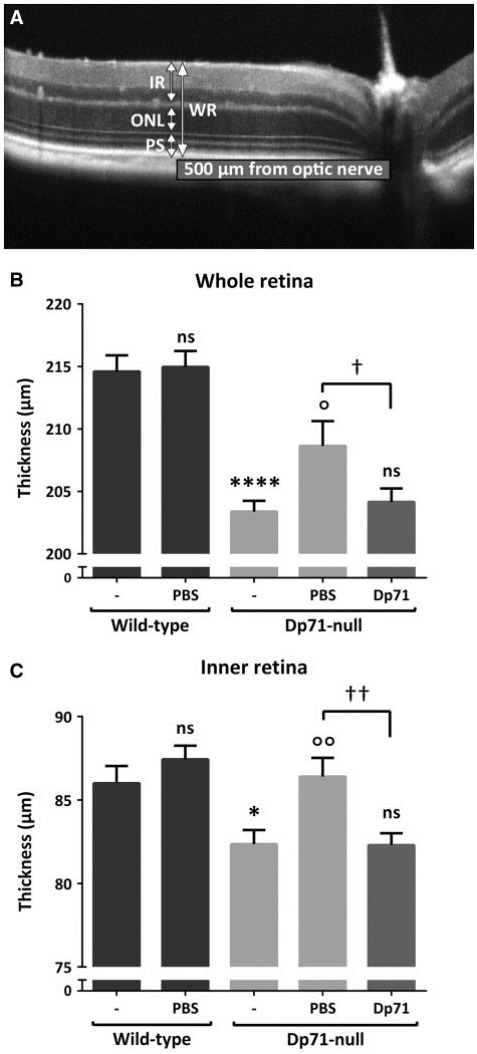

Figure 5. Reabsorption of induced retinal oedema in Dp71-null mice. Image A shows measurements performed on OCT images to evaluate the thickness of different retinal layers. Graphs B and C show the thickness of the whole retina (B) and of the inner retina (C) in wild-type and Dp71-null mice intravitreally injected with PBS or ShH10-GFP-2A-Dp71. Two months after PBS intravitreal injection, we observed a significant increase in the retinal thickness of Dp71-null mice but no modification in the wild-type retina. Dp71 restoration completely resorbed the retinal oedema caused by the needle intrusion. Bars represent means ± SEM for triplicate data points; n = 9. *P < 0.05, ****P < 0.0001 significant differences versus wild-type; P < 0.05, P < 0.01 significant differences versus wild-type; † P < 0.05, ††P < 0.01 significant differences versus Dp71-null (Mann-Whitney test).

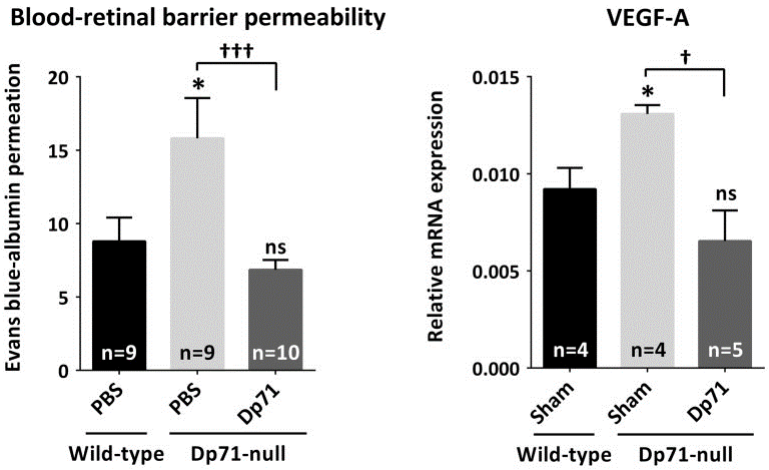

Figure 6. Restoration of the BRB permeability and of VEGF physiological expression in the Dp71-null mouse. BRB permeability was measured using Evans blue dye vascular permeability assay on WT and Dp71-null adult mice intravitreally injected with PBS or ShH10-GFP-2A-Dp71. Vascular permeability was strongly increased in Dp71-null mice compared to WT. However, Dp71-null mice with ShH10-GFP-2A-Dp71 present a normal BRB permeability compared to WT. Quantitative RT-PCR showed that VEGF-A mRNA expression was up-regulated in Dp71-null mice and that 2 months after ShH10-GFP-2A-Dp71 injection, VEGF wild-type expression level was restored. Bars represent means ± SEM for triplicate data points; n = 10 for BRB permeability and n = 5 for VEGF qPCR. *P < 0.05 significant differences versus wildtype; †††P < 0.001 significant differences versus Dp71-null (Mann-Whitney test).

Supplementary Material

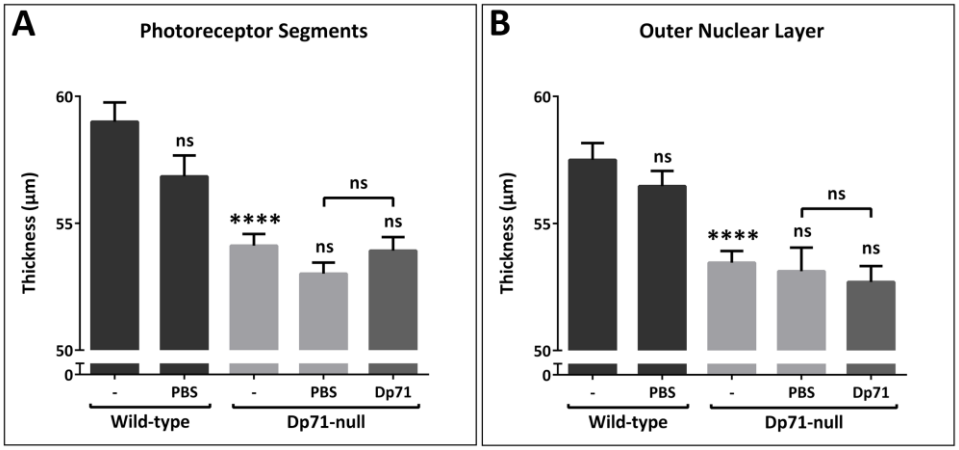

Figure S1. Measurements of retinal thickness on OCT images. Graphs A and B showed the thickness of the photoreceptor segments (A) and of the outer nuclear layer (B) in wild-type and Dp71-null mice intravitreally injected with PBS or ShH10-GFP-2A-Dp71. Bars represent means ± SEM for triplicate data points; n = 9. ****$p<0.0001$ significant differences versus wild-type (Mann Whitney test).

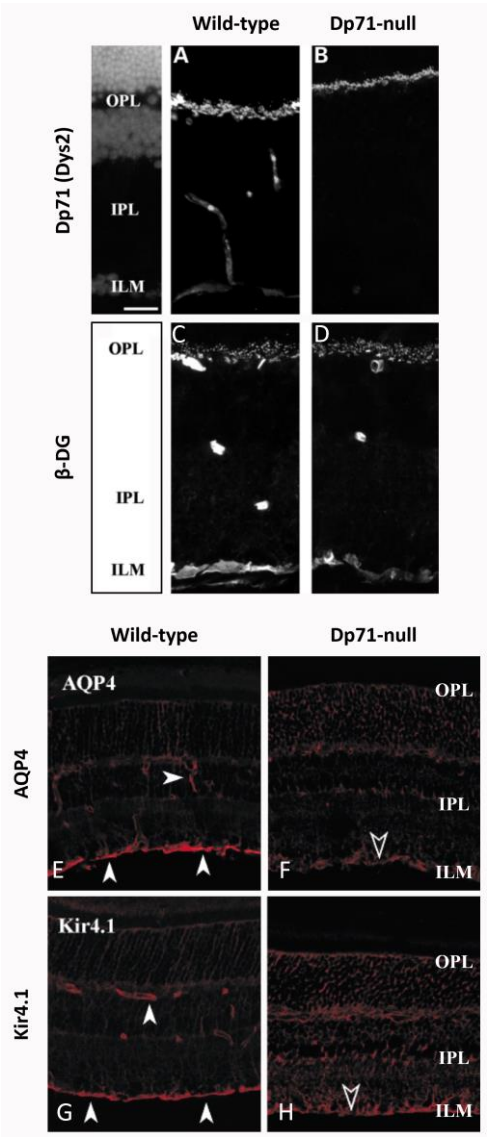

Figure S2. Immunohistochemistry of retinas from wild-type littermate (A, C) and Dp71-null mice (B, D) with antibodies against DMD gene products (A, B), β-dystroglycan (C, D), AQP4 (E, F) and Kir4.1 (G, H). Immunoreactivity with the Dys2 antibody revealed a signal at the ILM and around the blood vessels in wild-type retina (A), which was absent in the Dp71-null mice (B), while the signal observed at the OPL persisted. The staining with β-dystroglycan antibody decreased at the ILM from Dp71-null mice (D) compared to the wt (C). Top left side: the nuclear layers in a section of the same field were stained with DAPI (scale bar = 25 μm). Kir4.1 and AQP4 staining is distributed throughout the whole retina but strongly concentrated at the ILM and around the blood vessels (E and G, filled arrowheads). In Dp71-null retinas, Kir4.1 and AQP4 staining is more diffuse; note the dramatic diminution of the labeling at the ILM and around the blood vessels for both Kir4.1 and AQP4 (F and H, open arrowheads) as compared with the wt (E and G, solid arrowheads).

Abbreviations

AAV	Adeno-Associated Virus
AQP	Aquaporin
ARVO	The Association for Research in Vision and Ophthalmology
β-Dys	β-Dystroglycan
BRB	Blood Retinal Barrier
BSA	Bovine Serum Albumin
CBA	Chicken β-actin
CNS	Central Nervous System
DAPI	4',6-diamidino-2-phenylindole
DAPs	Dystrophin Associated Proteins
DGC	Dystrophin Glycoprotein Complex
DMD	Duchenne Muscular Dystrophy
Dp	Dystrophin
DR	Diabetic Retinopathy
ECL	Enhanced ChemiLuminescence
FIJI	Fiji Is Just ImageJ
GCL	Ganglion Cell Layer
GFAP	Glial Fibrillary Acidic Protein
GFP	Green Fluorescence Protein
INL	Inner Nuclear Layer
IPL	Inner Plexiform Layer
IR	Inner Retina
IS/OS	Inner Segment/Outer Segment
Kir	inwardly rectifying potassium channel
MacTel2	Macular Telangiectasia 2
MGC	Müller Glial Cell
NGS	Normal Growth Factor
OCT	Optical Coherence Tomography
ONL	Outer Nuclear Layer

OPL	Outer Plexiform Layer
PBS	Phosphate-buffered saline
PFA	Paraformaldehyde
PS	Photoreceptor Segments
PVDF	Polyvinylidene Difluoride
RT-PCR	Real Time Protein Chain Reaction
SD-OCT	Spectral Domain Optical Coherence Tomography
SEM	Standard Error of Mean
VEGF	Vascular Endothelial Growth Factor
WR	Whole Retina
WT	Wild-Type